Ag-Au superlattice band structure

T.-C. Chiang, T. Miller, and W. E. McMahon
Department of Physics, University of Illinois at Urbana-Champaign, 1110 West Green Street, Urbana, Illinois 61801-3080 and Materials Research Laboratory, University of Illinois at Urbana-Champaign, 104 South Goodwin Avenue, Urbana, Illinois 61801-2902
(Received 24 January 1994)

The dispersions of the *sp* bands in Ag-Au(111) superlattices are calculated. The calculation employs the nearly free-electron approximation for the wave functions within the Ag and Au layers. A one-band model for the superlattice band structure is developed and applied to the present system. This results in a simple analytic formula for the band dispersions of the superlattice geometry. The calculated band dispersions are in good agreement with experimental results determined previously by photoemission spectroscopy.

I. INTRODUCTION

The study of epitaxially grown multilayers and superlattices is an important field of research. A fundamental effect of the superlattice modulation in a crystal is the modification of its band structure. This leads to possibilities of band-structure engineering, which is an important concept in modern device and material design strategies. Although superlattices have been used in many applications, there remain many interesting scientific and technological issues to be investigated in detail. Specifically, there are few superlattice systems for which the electronic band dispersions $E(\mathbf{k})$ have been determined experimentally over a wide energy range. For metallic superlattices, the Ag-Au(111) system is one that has been investigated experimentally.[1,2] The measured energy dispersions of the *sp* band of this system show gaps caused by the superlattice modulation at the expected locations in the Brillouin zone.

Motivated by the availability of experimental data for Ag-Au(111) superlattices, we present in this paper a model calculation for this system. The purpose of this work is to illustrate some of the essential features of the superlattice electronic band structure as a function of the lattice modulation. Although modern first-principles calculations or simulations using large computers are capable of delivering this type of information, the complicated formalism and expensive execution tend to be overwhelming. The cost issue is especially critical when the superlattice unit-cell size becomes large. Our approach here is quite different. We use very simple models to solve the problem analytically, yielding an expression for the band dispersions of the superlattice in terms of the band parameters of the constituents. These analytic results can then be used to predict the general trend and behaviors as functions of the superlattice geometry. The system chosen for this study, Ag-Au(111) superlattices, has a particularly simple *sp* band for each of the two components,[3] making an analytic solution possible. Our results are fairly accurate, to within about ± 0.1 eV, as compared to the experiment. The simplicity of the analytic formalism and the numerically realistic results make this calculation of pedagogical value. The material presented here is suitable for use as a take-home problem for graduate courses in solid-state physics.

The main ingredients of our model calculation include the nearly free-electron approximation for the *sp* bands of Ag and Au, and a straightforward application of wave-function matching and the Bloch theorem at the layer boundaries. The model will be developed in Sec. II below. After that, we will make a comparison with available experimental data obtained by photoemission spectroscopy.

II. MODEL DEVELOPMENT

A. Nearly free-electron approximation for the *sp* band of Ag and Au

The *d* bands of Ag and Au are at a few eV below the Fermi level. Between the *d* bands and the Fermi level, the electronic states are mostly of *sp* character, and the band structure can be described quite well by the nearly free-electron approximation. Only two reciprocal-lattice vectors are needed in the Fourier expansion of the wave functions for a good description of this portion of the *sp* band. The method of nearly free-electron approximation can be found in any solid-state physics textbook. For a review of the application of the nearly free-electron method to the noble-metal band structures, we recommend the paper by Smith.[4] We will write down the basic formulas for the [111] direction in the following, mainly for the purpose of defining the notations and quantities relevant to our calculations. The wave-function $\phi(z)$ for either Ag or Au is given by

$$\phi(z)=\exp(ikz)+R\exp[i(k-g)z]\ , \tag{1}$$

where k is the wave vector, R is the ratio of coefficients between the two Fourier components, and $g\equiv 2p$ is the primitive reciprocal-lattice vector in the [111] direction. The relation between p (distance between the zone center and zone boundary, $k_{\Gamma L}$) and d (atomic layer spacing) is

given by

$$p = k_{\Gamma L} = \pi/d \ . \tag{2}$$

The Fourier expansion of the crystal potential is given by

$$U = V_g \exp(igz) + V_g \exp(-igz) \ , \tag{3}$$

where V_g is real. Working within the subspace spanned by $\exp(ikz)$ and $\exp[i(k-g)z]$, the eigenvalue equation for the energy E is given by

$$\begin{vmatrix} (\hbar^2/2m)k^2 - E & V_g \\ V_g & (\hbar^2/2m)(k-g)^2 - E \end{vmatrix} = 0 \ . \tag{4}$$

Solving this 2×2 determinant equation, we obtain the standard result

$$\epsilon(k-p) = E + \epsilon(p) - [V_g^2 + 4E\epsilon(p)]^{1/2} \ , \tag{5}$$

where $\epsilon(x) \equiv \hbar^2 x^2/2m$. This equation gives the wave vector k in terms of the energy E, i.e., the band dispersion. We also get

$$R = (E - \hbar^2 k^2/2m)/V_g \ , \tag{6}$$

which together with Eq. (1) gives the wave function as a function of E. An analysis of Eq. (5) shows that there is an "energy gap" of size $|2V_g|$ at $k = p$ (the L point in the Brillouin zone). Within this L gap, the wave vector k becomes complex, $k = p + i\eta$, and the solution given by Eq. (1) represents nonpropagating waves. The clean (111) surface supports a surface state, which is a nonpropagating solution that satisfies the vacuum boundary condition (see the paper by Smith[4] for a detailed discussion). This gap separates two branches of dispersion curves representing propagating waves with real k. For Au and Ag(111), the lower branch is occupied, and the upper branch is empty. The Fermi level lies within this gap.

The parameter V_g is determined by the size of the gap. For Ag(111), $|V_g| = 2.1$ eV.[5] A numerical evaluation of the above equations for the *sp* band of Ag near the gap shows a small but significant deviation from the experimental results (the curvature of the band does not match the experimental results). This is because the mixing with other bands is not totally negligible. A first-order correction of the above model to account for the "multiband effects" can be made to bring the model calculation and the experimental band dispersions into good agreement. This can be done by either adjusting the midgap energy position or by using an effective electron mass.[4] In our treatment here, we choose to use an effective electron mass $m = 0.74 m_e$, where m_e is the free-electron mass.[5] The energy reference $E = 0$ for our work will be the Fermi level. This is located at 0.33 eV above the lower edge of the L gap, so $E_L = -0.33$ eV for the lower edge. These three parameters E_L, V_g, and m provide a complete specification of the band dispersion and corresponding wave functions of the occupied *sp* states of Ag(111) relative to the Fermi level. The range of validity extends to about 4 eV below the Fermi level.[5]

The occupied branch of the Au(111) *sp* band near the Fermi level can be described well by a shift of the corresponding Ag dispersion by 0.77 eV toward higher binding energies. Thus $E_L = -1.1$ eV for Au(111), and the other two parameters V_g and m are taken to be the same as those for Ag(111).

The band dispersion does not depend on the sign of V_g. The sign comes into play when an interface is present in the system, because the phase of the crystal potential at the interface will depend on this sign. Here we choose the origin of our coordinate system midway between two (111) atomic planes, and with this choice $V_g = -2.1$ eV. This corresponds to the so-called Schockley-inverted case, and the wave function is p like (s like) at the lower (upper) edge of the gap.[4,6,7] If one chooses the origin at an atomic plane (as done by Smith[4]), the sign of V_g becomes positive. Our choice is more convenient for the superlattice geometry, because the boundary between neighboring Ag and Au layers is midway between two atomic planes.

Because of the reflection symmetry exhibited by U, the most general solution at a given energy E in either Ag or Au is a linear combination of $\phi(z)$ and $\phi(-z)$, where $\phi(z)$ is given by Eq. (1). Please note that taking the complex conjugate of ϕ does not necessarily yield an independent solution at the same E. For nonpropagating solutions, it is easy to show that $\phi^* \propto \phi$.

B. One-band model for the superlattice

By "one band," we mean that the superlattice band is synthesized from the *sp* band of Ag and Au only. Other bands (such as the *d* bands) are ignored. We will ignore the small difference in lattice constant between Ag and Au. Figure 1 defines the geometry of one period of the superlattice. The Ag (Au) slab consists of N_1 (N_2) atomic layers, and the origin is taken to be midway between the rightmost Ag atomic plane and the leftmost Au atomic plane. We will assume that the nearly free-electron wave functions given in Sec. II A are valid all the way to the boundary. This is not a bad approximation, since the metallic screening length is quite short in these metals (~ 0.5 Å). In other words, the boundary effect of the crystal potential does not propagate far into the metals.

We now construct the wave function of the superlattice. For simplicity, we will use subscripts 1 and 2 to denote Ag and Au, respectively. Instead of using $\phi(z)$ and $\phi(-z)$ directly, we use the symmetric combination $\phi_s = [\phi(z) + \phi(-z)]/2$ and the antisymmetric combination $\phi_a = [\phi(z) - \phi(-z)]/2$. The most general solution in the Ag slab at a given energy E is given by

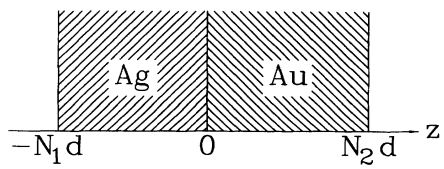

FIG. 1. The coordinate system and one period of the superlattice are shown. The origin is chosen to be at the Ag-Au interface. There are N_1 atomic layers of Ag to the left of the origin, and N_2 atomic layers of Au to the right. The interlayer spacing is d.

$$\psi_1 = a\phi_{1s}(z) + b\phi_{1a}(z) , \quad (7)$$

where a and b are arbitrary coefficients. A similar expression ψ_2 can be written for the Au slab. The wave function and its derivative must be continuous at $z=0$. Working out the algebra, it is easy to show that

$$\psi_2 = a[\phi_1(0)/\phi_2(0)]\phi_{2s}(z) + b[\phi_1'(0)/\phi_2'(0)]\phi_{2a}(z) , \quad (8)$$

where ϕ' denotes the first derivative of ϕ. The reason for using the symmetric and antisymmetric wave functions is that $\phi_s'(0)=0$ and $\phi_a(0)=0$, which leads to considerable simplification in the algebra for matching the boundary conditions.

We now apply the Bloch theorem to the superlattice geometry to link the wave functions and the first derivatives at $z=-N_1 d$ and $z=N_2 d$. Denoting the wave vector of the superlattice by q, we get

$$\psi_2(N_2 d) = \exp[iq(N_1+N_2)d]\psi_1(-N_1 d) , \quad (9)$$

$$\psi_2'(N_2 d) = \exp[iq(N_1+N_2)d]\psi_1'(-N_1 d) . \quad (10)$$

Applying the Bloch theorem to the Ag slab itself, we get

$$\begin{aligned}\psi_1(-N_1 d) &= a[\phi_1(-N_1 d)+\phi_1(N_1 d)]/2 \\ &\quad + b[\phi_1(-N_1 d)-\phi_1(N_1 d)]/2 \\ &= a\cos(k_1 N_1 d)\phi_1(0) \\ &\quad - ib\sin(k_1 N_1 d)\phi_1(0) , \end{aligned} \quad (11)$$

where we have used $\phi_1(\pm N_1 d) = \exp(\pm ik_1 N_1 d)\phi_1(0)$. Similarly,

$$\begin{aligned}\psi_1'(-N_1 d) &= -ia\sin(k_1 N_1 d)\phi_1'(0) \\ &\quad + b\cos(k_1 N_1 d)\phi_1'(0) . \end{aligned} \quad (12)$$

One can easily derive similar expressions for the Au; that is, one can express $\psi_2(N_2 d)$ and $\psi_2'(N_2 d)$ appearing in Eqs. (9) and (10) in terms of $\phi_2(0)$ and $\phi_2'(0)$. With these substitutions, Eqs. (9) and (10) become a pair of linear homogeneous equations in a and b. The resulting quadratic secular equation for $\exp[iq(N_1+N_2)d]$ can be solved in a straightforward manner, which yields q in terms of E, namely the band dispersion for the superlattice. The result is

$$\begin{aligned}&\cos[q(N_1+N_2)d] \\ &\quad = \cos(k_1 N_1 d)\cos(k_2 N_2 d) \\ &\qquad - [(\chi+1/\chi)/2]\sin(k_1 N_1 d)\sin(k_2 N_2 d) , \end{aligned} \quad (13)$$

where

$$\chi = \phi_1'(0)\phi_2(0)/[\phi_1(0)\phi_2'(0)] . \quad (14)$$

Equation (13), based on the application of the Bloch theorem, is a fairly general result, and does not depend on the nearly free-electron approximation. For the Ag-Au superlattice considered here, we can use Eq. (1) to evaluate χ, and obtain

$$\chi = \{k_1 - p[2R_1/(1+R_1)]\}/\{k_2 - p[2R_2/(1+R_2)]\} . \quad (15)$$

Our computation of the superlattice band dispersion begins with Eqs. (5) and (6), which give k and R in terms of E, respectively. These are then plugged into Eq. (15) to get χ, and finally Eq. (13) yields q in terms of E. Real solutions of q give rise to propagating waves, while complex solutions can be found in "gaps" which are important for surface and interface states if additional boundaries are present in the system. In our discussion of the results, we will concentrate on the real solutions which correspond to band dispersions.

III. COMPARISON WITH DATA

There exist two reports on the experimental band dispersions of Ag-Au(111) superlattices in the literature.[1,2] The data were obtained by angle-resolved photoemission spectroscopy using the light source at the Synchrotron Radiation Center of the University of Wisconsin-Madison. The experimental details will not be discussed here. The more recent of these two reports[2] has a better signal-to-noise ratio, and the data are of higher quality. Therefore, we will concentrate our discussion on this one first. The system investigated is an Ag-Au(111) superlattice with a period of 12 monolayers (ML), which consists of 8 ML Ag and 4 ML Au. For simplicity, we will refer to this system as the (8+4) superlattice, and $N_1=8$ and $N_2=4$ in our notation. Figure 2 shows the result of our computation. The occupied Ag and Au sp band dispersions are indicated by dashed curves for comparison. The calculated superlattice band, presented in the extended zone scheme, is shown by the solid curves. It falls between the Ag and Au band dispersions, as expected intuitively. It is closer to the Ag dispersion, because the system is overall Ag rich. The theoretical superlattice band exhibits two gaps of 0.298 and 0.114 eV at

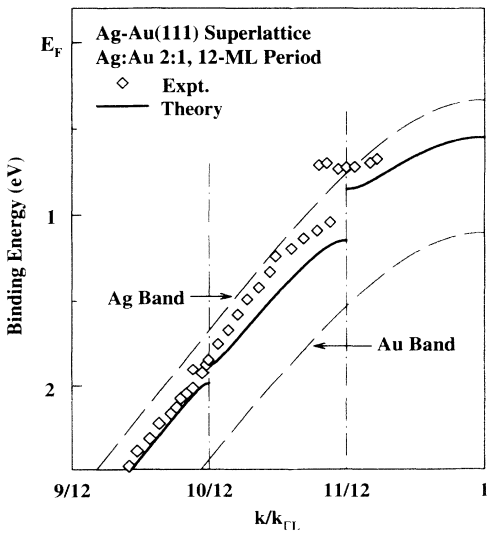

FIG. 2. Band dispersion curves of Ag, Au, and an (8+4) Ag-Au superlattice along the [111] direction, displayed within the first zone of Ag (Au). The theoretical superlattice dispersion curves are indicated by the solid curves. The diamonds are data points.

$k/p = \frac{11}{12}$ and $\frac{10}{12}$, respectively. These positions in the Brillouin zone correspond to the superlattice zone boundaries, and are indicated by the vertical dash-dotted lines in the figure. Also show in this figure are the data, indicated by diamonds. The upper gap at $k/p = \frac{11}{12}$ is clearly seen. The lower gap at $k/p = \frac{10}{12}$ is not apparent due to its small size and noise in the data. However, if one views the data at a glancing angle to the paper surface, it is clear that there is a kink and offset at the correct location, which is indicative of a small gap.

The upper branch of the data near $k/p = \frac{11}{12}$ shows a parabolic shape extending to k/p less than $\frac{11}{12}$. This is related to the nature of the photoemission band-mapping technique.[1] What the experiment provides is a band structure in the repeated zone scheme, although the peak intensity is not necessarily detectable everywhere. To make a better comparison between the theory and experiment, we replot the data and calculation in Fig. 3 using the reduced zone scheme. Here, one sees that the *sp* band is folded into three branches. The data are somewhat higher than the theory for all three branches, and the average deviation is about 0.1 eV. The overall agreement in the shapes of the bands is very encouraging. For the lowest branch, we show a dashed curve through the data, which is just the theoretical curve shifted up by 0.05 eV. With this shift, it describes the data well. Similarly, we find a shift of 0.11 eV for the top branch, as indicated by the dashed curve. For the middle branch, the shift is not a constant, and therefore we cannot simply make a rigid upward shift of the theoretical curve. The dashed curve shown in the figure is a sixth-order polynomial fit to the data. This polynomial is constrained to have zero slopes on both ends, and thus the number of free parameters is five. This represents the minimum number of parameters for a fit to a curve of this shape, because one needs to account for five basic features including the heights of the two ends of the curve (two parameters), the curvatures near the two ends (two parameters), and the point at which the curvature changes from concave to convex (one parameter). In our fit, we have ignored the data point very close to $k = 0$ in Fig. 3 because the photoemission data here are likely an unresolved convolution of two peaks derived from both the middle branch and the bottom branch (the resolution of the photoemission experiment is about 0.1 eV, and the peaks are further broadened by lifetime effects). The dashed curves in Fig. 3 are thus fair representations of the data. Based on this analysis, we obtain the experimental band gaps as 0.30 and 0.12 eV, with an estimated error of no larger than ± 0.05 eV. These numbers are very close to the theoretical values of 0.298 and 0.114 eV mentioned above.

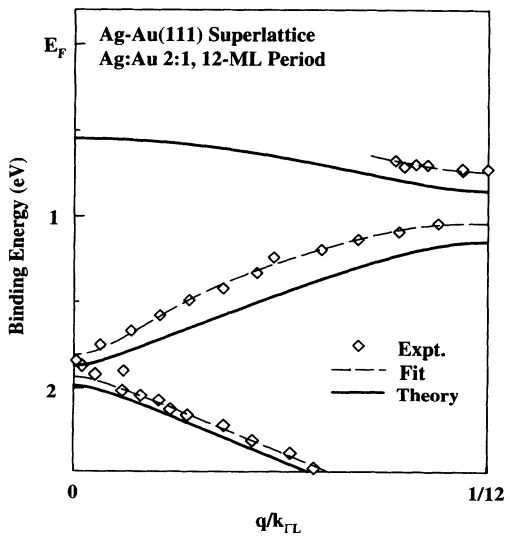

FIG. 3. The theoretical and experimental band dispersions for the (8+4) superlattice are shown in the reduced zone.

The agreement between theory and experiment is quite good, considering that state-of-the-art, first-principles calculations of band structures often exhibit errors larger than what we have here. The good agreement is due in part to our use of the experimental band dispersions of Ag and Au, and in a sense our model is an interpolation based on known results. We now comment on sources of error in our model. Equation (13) is exact within the one-electron, one-band picture. The one-band approximation will likely introduce some error, but the largest error is likely in the computation of χ. The nearly free-electron model is obviously not the most accurate method for generating the wave functions, for which higher harmonics, although small in magnitude, should have been retained. Also, there is some error in assuming that the Ag and Au wave functions can be used all the way to the boundary without modification by the boundary potential which must have a finite extent. However, we are unable to quantify these discussions, as more accurate calculations are unavailable at this time.

There is another, earlier report on the superlattice band structure of Ag-Au, as mentioned above.[1] The data, with more noise, were not of as high quality as those shown in Figs. 2 and 3. Nevertheless, the overall shapes of the bands from the calculation are in good agreement with the data. Differences similar to those seen in Fig. 2 are observed. For brevity, we will not show the corresponding figures. We will just give the values of the band gaps. For the (6+6) system, the measured upper gap is 0.28 ± 0.1 eV, and the theoretical value is 0.360 eV. The lower gap is zero based on the data, and the theoretical value is 0.006 eV, which is too small to be observed experimentally. For the (4+4) system, the measured upper gap is 0.37 ± 0.1 eV, and the theoretical value is 0.270 eV. The lower gap was not accessible in the experiment. Thus all of the experimental results are in agreement with the theory within the experimental errors.

For reference purposes, we show in Fig. 4 the calculated band-edge energies for superlattices with a 12-ML period. The abscissa is the thickness of the Ag slab within one period; when it is zero (12), the system is pure Au (Ag). The results for $k/k_{\Gamma L} = 1$ (in terms of the original zone) represent the variation of the valence-band maximum. It is at 1.1 eV for pure Au, and rises to 0.33 eV for Ag. The variation is fairly linear, with a small upward bowing. The point at $k/k_{\Gamma L} = \frac{11}{12}$ for the pure material is split to form a gap for the superlattice (the upper

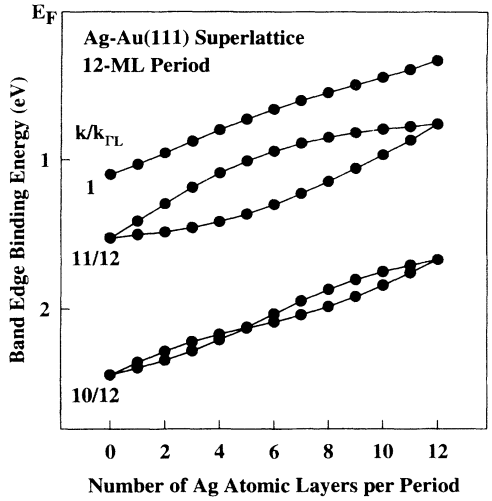

FIG. 4. Theoretical band-edge energies as a function of the Ag slab thickness for a 12-ML period superlattice. The uppermost curve shows the variation of the valence-band maximum at the L point. The two curves below show the variation of the gap at $k/k_{\Gamma L}=\frac{11}{12}$, and the bottom two curves show the variation of the gap at $k/k_{\Gamma L}=\frac{10}{12}$.

gap). As expected, the gap is the largest with about equal Ag and Au slab thicknesses at which the superlattice modulation has the largest Fourier component. The lower gap at $k/k_{\Gamma L}=\frac{10}{12}$, however, shows a very different behavior. It is zero at about equal Ag and Au slab thicknesses. This is not surprising. Within the nearly free-electron model, the gap is just twice the appropriate Fourier coefficient of the crystal potential. The upper gap is related to the reciprocal-lattice vector of $11g_s=g-g_s$ where $g_s=g/12$ is the primitive reciprocal-lattice vector of the 12-ML superlattice, and the lower gap is related to $10g_s$. If one considers the Ag-Au superlattice modulation as a square-well-type potential in a crude approximation, it is easy to see that such a potential, if the up and down parts are of equal thickness, will have no even harmonics (the potential is an odd function). Thus the second gap has to be zero for symmetry reasons. In our model, the potential is not a simple square-well-type potential, and so the point at which the gap vanishes does not happen exactly at the (6+6) configuration. Rather, it happens approximately at the (5+7) configuration. Because of the existence of this "node" for the lower gap as a function of the Ag a slab thickness, the gap is generally smaller.

IV. SUMMARY AND CONCLUSIONS

This study is a model calculation of the *sp* band structure of Ag-Au(111) superlattices. The model employs some basic ideas in solid-state physics, i.e., the nearly free-electron approximation and the Bloch theorem. The results are expressed in terms of simple analytic functions, and agree well with the experimental data, to within about 0.1 eV. This is one of the few systems in which the band structure can be calculated analytically with numerically realistic predictions. For this reason, this system and the calculation can serve as models to illustrate the general electronic behaviors of superlattices.

ACKNOWLEDGMENTS

This material is based upon work supported by the U.S. National Science Foundation under Grant No. DMR-92-23546. Acknowledgment is made to the Donors of the Petroleum Research Fund, administered by the American Chemical Society, and to the U.S. Department of Energy (Division of Materials Sciences, Office of Basic Energy Sciences), under Grant No. DEFG02-91ER45439, for partial equipment and personnel support in connection with the beam line operation, and for the Department of Energy's support of the central facilities of the Materials Research Laboratory of the University of Illinois. The Synchrotron Radiation Center of the University of Wisconsin-Madison is supported by the U.S. National Science Foundation.

[1]T. Miller, M. A. Mueller, and T.-C. Chiang, Phys. Rev. B **40**, 1301 (1989).

[2]T. Miller and T.-C. Chiang, Phys. Rev. Lett. **68**, 3339 (1992).

[3]For an overview of the electronic band structure of noble metals, see N. W. Ascroft and N. D. Mermin, *Solid State Physics* (Holt, Rinehart, and Winston, Philadelphia, 1976), pp. 288–297.

[4]N. V. Smith, Phys. Rev. B **32**, 3549 (1985).

[5]M. A. Mueller, T. Miller, and T.-C. Chiang, Phys. Rev. B **41**, 5214 (1990).

[6]O. Madelung, *Introduction to Solid State Theory* (Springer-Verlag, New York, 1978), pp. 426–428.

[7]J. E. Inglesfield and B. W. Holland, in *The Chemical Physics of Solid Surfaces and Heterogeneous Catalysis,* edited by D. A. King and D. P. Woodruff (Elsevier, New York, 1981), Vol. 1, pp. 196–204.